## Supporting Information for "Revealing Protein Structures in Solid-phase Peptide Synthesis by ^{13}C Solid-state NMR: Evidence of Protein Misfolding for Alzheimer's β"

by Songlin Wang[1)] and Yoshitaka, Ishii[1,2)]

1) *Department of Chemistry, University of Illinois at Chicago, 845 West Taylor Street, Chicago, Illinois 60607.*

2) *Center for Structural Biology, University of Illinois at Chicago, 1100 South Ashland Street, Chicago IL 60607*

### References with complete citations for refs. 2(a) and 12(b):

(2a)   Beyer, M.; Nesterov, A.; Block, I.; Konig, K.; Felgenhauer, T.; Fernandez, S.; Leibe, K.; Torralba, G.; Hausmann, M.; Trunk, U.; Lindenstruth, V.; Bischoff, F. R.; Stadler, V.; Breitling, F. *Science* **2007**, *318*, 1888-1888.

(12b)     Noguchi, A.; Matsumura, S.; Dezawa, M.; Tada, M.; Yanazawa, M.; Ito, A.; Akioka, M.; Kikuchi, S.; Sato, M.; Ideno, S.; Noda, M.; Fukunari, A.; Muramatsu, S.; Itokazu, Y.; Sato, K.; Takahashi, H.; Teplow, D. B.; Nabeshima, Y.; Kakita, A.; Imahori, K.; Hoshi, M. *J. Biol. Chem.* **2009**, *284*, 32895-32905.

### Supplementary Experimental Details

#### Peptide synthesis and sample packing

All starting materials, with the exception of isotope-labeled Fmoc-protected amino acids, were obtained from commercial suppliers and used without further purification. All of the unlabeled Fmoc-protected amino acids, HCTU, and low-density Fmoc-Val-Wang resin (0.22 meq/g) were obtained from Peptides International (Louisville, KY). Uniformly [13]C- and ^{15}N-labeled amino acids were purchased from Isotec/Sigma-Aldrich (Miamisburg, OH). The Fmoc protection of the labeled amino acids was performed at the UIC Research Resource Center.[1] Piperidine was purchased from Sigma-Aldrich (St. Louise, MO). Other reagents and solvents for peptide synthesis were purchased from Applied Biosystems (ABI, Foster City, CA).

For the ^{13}C SSNMR experiments, selectively [13]C- and ^{15}N-labeled Aβ(1-40) samples were synthesized with standard Fmoc-based synthesis as reported previously[2-3] with an ABI 433 peptide synthesizer using low-density Fmoc-Val-Wang resin (0.22 mmol/g).  The selective isotope labeling with uniformly [13]C-, ^{15}N-amino acids was introduced at several residues (Phe-19, Val-24, Gly-25, Ala-30, Leu-34 or Ala-2, Phe-4, Val-12) in Aβ(1-40). The standard Fmoc synthesis protocol was employed with capping with acetic anhydride after each coupling step.   The capping protocol terminated any unreacted peptide terminus after

a coupling step with acetyl group, and this allowed us to profile resides that display incomplete coupling in the synthesis if any.   The resin was swollen by dichloromethane (DCM), and then *N*-Methyl-2-pyrrolidone (NMP) was used as solvent during the synthesis. To prevent any incomplete coupling at the N-terminus residues, Ala-2, Glu-3, Phe-4 were coupled twice, and Asp-1 was coupled four times in SPPS, as incomplete couplings were noticeable for these residues with single coupling.   The purity of the peptides was tested by mass spectroscopy as will be discussed below.     The resin was washed by DCM at the end of the synthesis to replace NMP in order to minimize the risk of using flammable NMP for SSNMR experiments.

The resin-bound peptide sample solvated with DCM was packed into a 2.5-mm MAS rotor without further drying, and then immediately tested for sample spinning for SSNMR MAS experiments.   The NMR spectra were acquired after the spinning became stable. The overall time for packing the sample and testing spinning was about 1-4 hours.   For the samples solvated with DCM, the total sample amount in the rotor was about 18 mg, which included resin-bound peptides of 4.5-5.0 mg and DCM in rotors.   For the dried resin-bound peptide sample, the sample containing solvent was placed under vacuum until the solvent was removed.   The sample amount was about 9.2-9.6 mg.   Unless otherwise mentioned, all the SSNMR spectra of this study were normalized by the amount of the resin-bound peptide in the rotors for comparison and quantitative analysis.
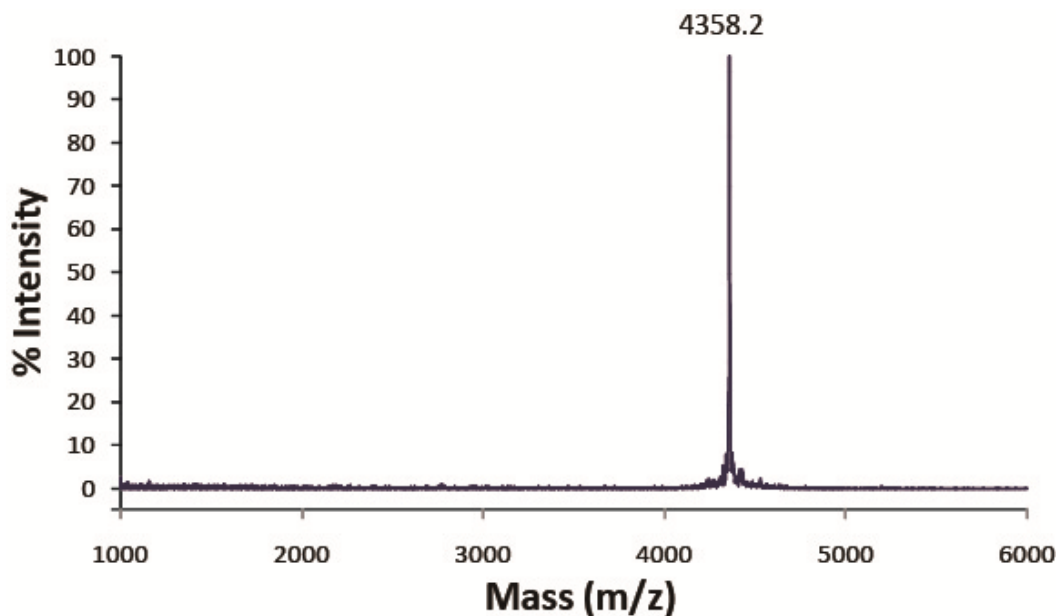


**Figure S1.** The mass spectroscopic analysis of (a) Aβ(1-40) labeled at Phe-19, Val-25, Gly-25, Ala-30 and Leu-34.   The sample was used for the data in Fig. 1.

**Mass spectrometry analysis for confirmation of sample homogeneity**

The homogeneity of the labeled peptides was tested by mass spectrometry as shown in Fig. S1 for Aβ(1-40) labeled at Phe-19, Val-24, Gly-25, Ala-30 and Leu-34.   The peptide was cleaved from resin as discussed previously,[2-3] and the cleaved peptide was lyophilized for the mass analysis without further purification.   In Fig. S1a, the major peak at m/z of 4358.2 is attributed to Aβ(1-40) labeled at Phe19, Val-24, Gly-25, Ala-30 and Leu-34 (molar mass: 4359.9) within the experimental error (ca. ±2).   The mass spectrum indicates very little other peptide species or impurities.   Similarly, the purity for the other labeled Aβ(1-40) sample was confirmed by mass analysis.   Overall, the mass spectrometry results show high homogeneity for the resin-bound peptide samples that were analyzed in this NMR study.

In contrast, noticeable incomplete coupling was observed if single coupling was used in the N-terminus of Aβ(1-40).   Also, we found that a synthesis protocol similar to the one used here resulted in the incomplete coupling at the end of the sequence for Aβ(1-40) at different automated peptide synthesizers such as a Protein Technologies Prelude system.   This suggests that SPPS of Aβ(1-40) may be considerably difficult without optimization, depending on an instrument and a synthesis method used.

**Solid-State NMR Experiments**

All the SSNMR experiments were conducted at a static field of 9.4 T using a Varian InfinityPlus 400 NMR spectrometer and a home-built 2.5-mm magic angle spinning (MAS) triple-resonance probe. The $^{13}$C chemical shifts were referenced to TMS using adamantine CH signal (38.56 ppm) as the secondary external reference. The MAS spinning speed was set to 20,000 ± 3 Hz for all of the experiments.   The cooling air temperature for a Varian variable-temperature stack was set at -15 °C, and the sample temperature was approximately 9 °C in this condition.   For the 1D CPMAS experiment in Fig. 1, during the cross-polarization (CP) period, the $^{13}$C radio-frequency (RF) field amplitude was linearly swept from 46 to 63 kHz during a contact time of 1.0 ms, while the $^{1}$H RF amplitude was kept constant at 76 kHz.   For each spectrum, 256 scans of time-domain signals were accumulated with recycle delays of 4 s and acquisition time of 10 ms under $^{1}$H TPPM decoupling[4] at 88 kHz.   A Gaussian window function of 100 Hz was applied for processing.

In the 2D $^{13}$C/$^{13}$C chemical-shift correlation experiments in Fig. 1-2, the finite pulse RF driven recoupling (fpRFDR) pulse sequence was employed.[5]   During the CP period, the $^{13}$C RF field amplitude was linearly swept from 46 kHz to 62.5 kHz during a contact time of 1.0 ms while the $^{1}$H RF amplitude was

kept constant at 76 kHz. During a mixing period, fpRFDR $^{13}$C-$^{13}$C dipolar recoupling sequence with a mixing time of 1.6 ms and a $^{13}$C π-pulse width of 15 μs was used. $^1$H TPPM decoupling of 90 kHz was employed during the $t_1$ and $t_2$ periods, while cw decoupling of the same amplitude was used during the mixing period. The 2D data were processed with a 50-Hz Lorentz-to-Gauss transformation window function, and an additional 135-Hz Gaussian window function along the $t_1$ and $t_2$ periods before Fourier transformation.

A $^1$H-$^{13}$C REDOR pulse sequence (Fig. S2) was used to determine the mobility of peptides bound to resin. During the CP period, the $^{13}$C RF field amplitude was linearly swept from 45 kHz to 73.2 kHz during a contact time of 1.0 ms while the $^1$H RF amplitude was kept constant at 79 kHz. After the CP, the signal was subject to dephasing due to $^1$H-$^{13}$C dipolar interaction restored by $^{13}$C-$^1$H REDOR. After the dephasing period, $^{13}$C signals were acquired under $^1$H TPPM decoupling of 90 kHz. When the effective dephasing time of τ is set to 0 in the $^{13}$C-$^1$H REDOR sequence, a spin echo is formed with little dephasing due to $^{13}$C-$^1$H dipolar couplings under the fast MAS condition; this yields a control $^{13}$C signal intensity of $I_0$ = $I(0)$. As we increased τ of $N\tau_R/9$ ($N$ = 0, 1 ,2 ,3, 4), the signal intensity $I(\tau)$ was decreased by $^1$H-$^{13}$C dipolar couplings, where $\tau_R$ denotes a rotation period ($\tau_R$ = 50 μs). When the $^1$H π-pulse is placed at the middle of the rotor cycle at $N$ =4, the signal should be most dephased. $^{13}$C and $^1$H π-pulse widths of 5.56 μs or $\tau_R/9$ were used.
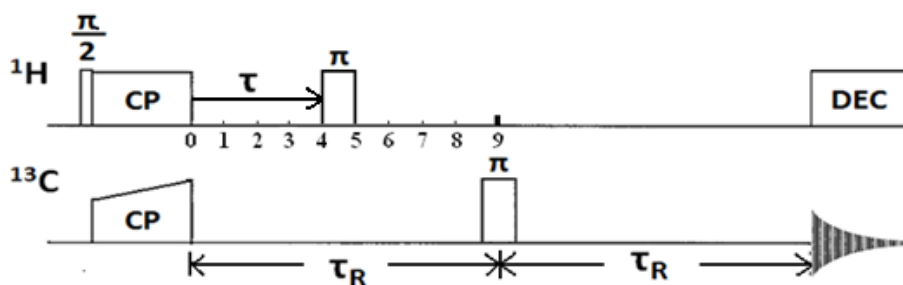


**Figure S2**. The pulse sequence for $^1$H-$^{13}$C REDOR experiments. Initial $^{13}$C magnetization was prepared by a ramped cross-polarization. The data were collected for five dephasing periods as τ = $N\tau_R/9$ ($N$ = 0, 1, 2, 3, 4) for different positions of the $^1$H π-pulse. When $N$ = 0, the sequence yields a spin echo with minimal dipolar dephasing due to the $^{13}$C-$^1$H dipolar couplings. When the π-pulse is at the middle of the rotor cycle at $N$ =4, the signal would be most dephased by the $^{13}$C-$^1$H dipolar couplings.

## Spectral simulation for CH-REDOR experiments

Simulations for the $^1$H-$^{13}$C REDOR experiment were performed by SPINEVOLUTION software.[6] The dipolar dephasing efficiency reflects the local dynamics of the chemical group.

We used order parameter $S$ to quantitatively examine the mobility. We simulated the dipolar dephasing curves for an isolated $^{13}C$-$^1H$ spin system for different order parameter $S$ using a $^{13}C$-$^1H$ bond length ($r_0$ = 1.12 Å), and then compared the dephasing curves with the experimental results. As dipolar coupling is proportional to $1/r^3$, in the SPINEVOLUTION software, simulations for dipolar couplings scaled by $S$ were implemented by performing simulation for different $^{13}C$-$^1H$ distances of $r = r_0/S^{1/3}$.

**Supplementary Data**

**1D $^{13}C$ CPMAS Spectra of Val-Wang Resin**

Control spectra of resin samples were collected for analyzing the spectra of Aβ peptides bound to resin. Figure S3 shows CPMAS spectra of Val-Wang resin (a) without solvent and with (b) dichloromethane and (c) NMP. The resin was used for the SPPS of the Aβ samples. The spectra were collected with the same number of scans, and the signal intensities were normalized by the amount of the resin for comparison. The intensities of the peaks are much higher for the sample without solvent (Fig. S3a), compared with those for the samples containing (b) DCM or (c) NMP. The intensity change is likely to be attributed to the mobility of the poly-styrene resin. The resin was swollen in DCM or NMP and the diameter of resin was increased about 1.5 times after soaked in solvent. We observed that the signal intensities for the resin were recovered after the solvent was removed from the resin.
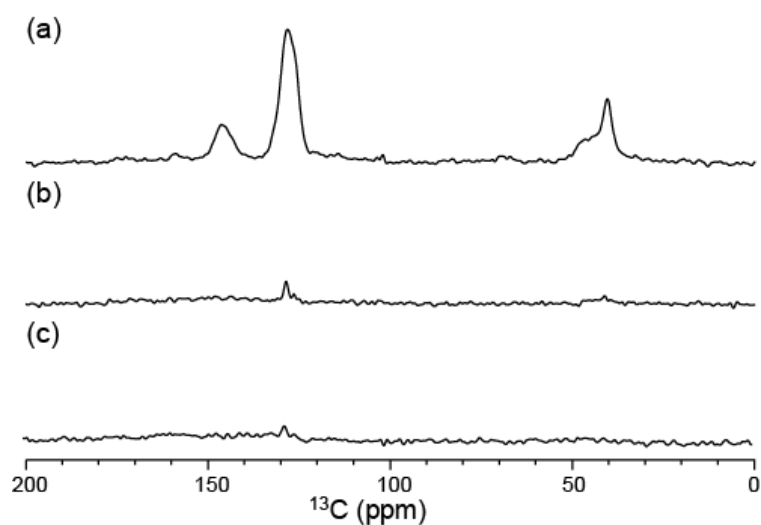


**Figure S3.** (a-c) $^{13}C$ CPMAS spectra for Val-Wang resin in (a) no solvent, (b) DCM, (c) NMP. The spectra were acquired with 256 scans with the experimental times of 17 min., and displayed in the same scale.
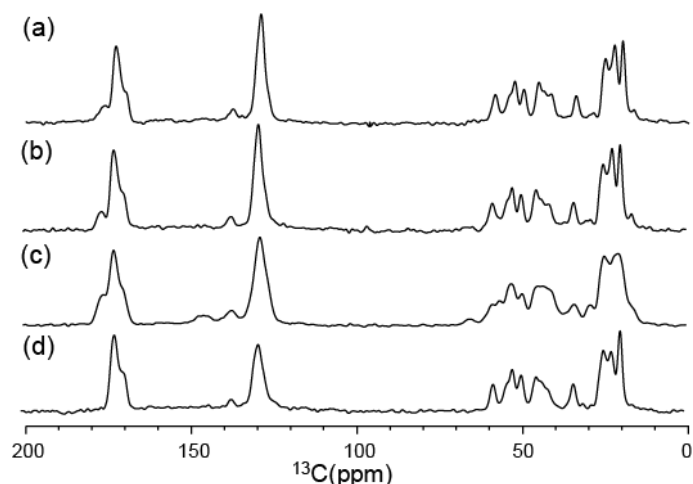
**Figure S4.** (a-d) ¹³C CPMAS spectra for Aβ(1-40) bound to resin in different condition. The Aβ(1-40) peptide was uniformly ¹³C- and ¹⁵N- labeled at Phe19, Val-24, Gly-25, Ala-30 and Leu-34. (a, b) ¹³C CPMAS spectra measured for the sample in DCM at 2 h and at 112 h after the synthesis was complete.  (c) A ¹³C CPMAS spectrum of the same sample measured after all the solvents have already evaporated.  (d) A ¹³C CPMAS spectrum of the same sample measured after dried resin-bound peptide was resolvated with NMP.  The signal intensities were normalized by the amount of the sample used for comparison.  Each spectrum was collected with 256 scans, and the experimental times was 17 min.

## Time and solvent dependence of ¹³C CPMAS spectrum of resin-bound Aβ(1-40).

Figure S4 (a, b) shows ¹³C CPMAS spectra of resin-bound Aβ(1-40) that was uniformly ¹³C- and ¹⁵N-labeled at Phe19, Val-24, Gly-25, Ala-30, Leu-34 in DCM (a) 2 h and (b) 112 h after the synthesis was complete.  In fact, no spectral changes were observed for several days as long as the sample was solvated in DCM.  The data were acquired with 256 scans for the samples solvated with DCM.  The spectral difference is very minor; especially ¹³C chemical shifts indicate that the structure of the resin-bound peptides is unchanged over time right after the synthesis.  Figure S4c shows a spectrum of the same sample, but after the DCM was removed by drying.  When the DCM was removed, the line widths became mildly increased.  This is probably because the conformations of the peptides show some heterogeneity as the local motions of the peptide is restricted after drying. Nevertheless, the positions of the chemical shifts are basically unchanged, suggesting that the average conformations of the peptide are unchanged after drying. Figure S4d shows a ¹³C CPMAS spectrum of the same sample after resolvated with NMP.  Spectral features similar to those in Fig. S4(a,b) were recovered with slightly better resolution.  Since the shift positions are essentially identical with those in Fig. S4(a,b), the results indicate that the structure of Aβ(1-40) bound to resin is independent of the solvents.  We also confirmed that the sample resolvated with DCM show an identical spectrum with Fig. S4a.
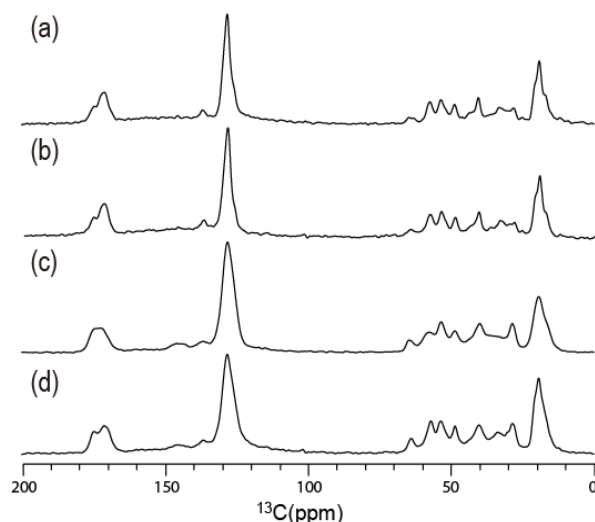
**Figure S5**. (a-d) $^{13}$C CPMAS spectra for resin-bound Aβ(1-40) that was uniformly $^{13}$C- and $^{15}$N- labeled at Ala-2, Phe-4 and Val-12 in different conditions. (a, b) $^{13}$C CPMAS spectra measured for the sample in DCM at 1 hours and at 80h after the synthesis was complete. (c) A $^{13}$C CPMAS spectrum of the same sample measured after the solvent was evaporated. (d) A $^{13}$C CPMAS spectrum of the same sample measured after dried resin-bound peptide was resolvated with NMP. Each spectrum was collected with 1024 scans. The experimental times were 68 min each.

Figure S5 (a, b) show $^{13}$C CPMAS spectra of Aβ(1-40) labeled at Ala-2, Phe-4 and Val-12, (a) 1h and (b) 80 h after the synthesis was complete. The chemical shifts and signal intensities of these spectra are very similar, suggesting that the peptide structure was unaltered over time. However, when the solvent was removed, some new peaks emerged as shown in Fig. S5c (and see a 2D spectrum in Fig. 2c). These results suggest the presence of the second conformers without solvent. Compared with the solvated sample, the integral intensity in the aliphatic region (10-70 ppm) of the dried sample is about 140% when the intensity was normalized by the sample amount and the scan numbers. A plausible explanation is that the second conformer was highly dynamic in the N-terminal region in the presence of the solvent, and thus the signal was not observed with solvent due to the lower transfer efficiency in cross polarization caused by higher mobility. When the solvent was removed, the second component gained SSNMR signal intensities due to restricted dynamics. Figure S5d shows $^{13}$C CPMAS spectrum for the same sample after the dried sample was resolvated with NMP. Besides slightly improved resolution, the spectrum shows very similar features to those in Fig. S5(a, b) solvated with DCM.
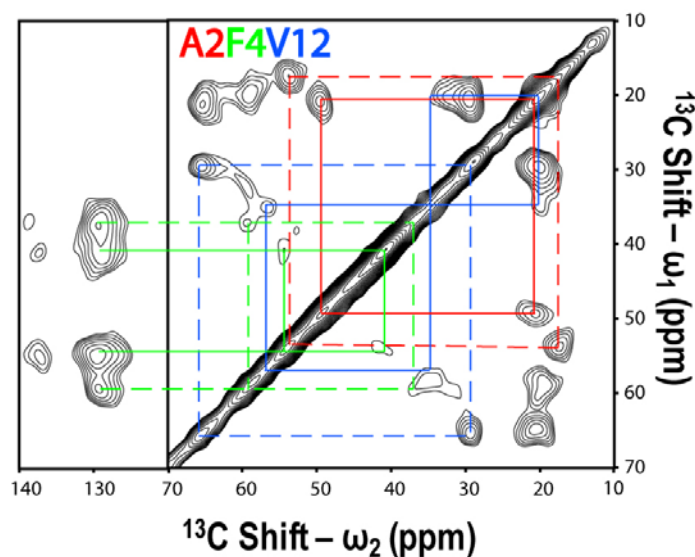
**Figure S6**. 2D $^{13}$C/$^{13}$C DARR spectrum of a resin-bound Aβ(1-40) sample without solvent. The Aβ peptide was labeled at Ala-2, Phe-4, and Val-12. The solid lines show the resonances of the β-sheet component while the dashed lines show the resonances of the α-helical component. The mixing time was 50 ms. The MAS spinning speed was set to 20 kHz. The experimental time was 20 h.

**Dipolar assisted rotational resonance (DARR) NMR experiment for resin-bound Aβ(1-40).**

Since the $^{13}$C$_\alpha$/$^{13}$C$_\beta$ cross peaks of the α-helical component of Phe-4 partially overlap with those of the β-sheet component of Val-12 in the aliphatic region, DARR experiment[7] was used to confirm the chemical shifts of the α-helical component of Phe-4 through the side chain connectivities. For the DARR mixing, $^1$H rf field was irradiated at $\omega_{1H} = \omega_R$ in the rotary resonance condition with a mixing time of 50 ms, where $\omega_{1H}$ denotes the $^1$H rf field intensity for the DARR mixing. With this mixing condition, intra-residue connectivities are typically observed. As shown in Fig. S6, the cross peaks between Phe-4 side chains show the connectivities with two types of $^{13}$C species (α-helical & β-strand) for each of $^{13}$C$_\alpha$ and $^{13}$C$_\beta$. The peaks for the β-sheet component of Phe-4 indicated by solid green line (Fig. S6) confirm the assignment by the fpRFDR experiment in Fig. 2c. The peaks for the α-helical component indicated by dashed green lines can be clearly assigned with the correlations from the aromatic side-chain resonances at ~128 ppm to $^{13}$C$_\beta$ at 59.4 ppm or $^{13}$C$_\beta$ at 37.1 ppm for Phe-4. The chemical shifts data are summarized in Table S1.

**Quantitative analysis of dynamic properties of resin-bound Aβ(1-40) in SPPS**

Dynamic properties of proteins are fundamental parameters that define their functionality. In SPPS, the dynamics are likely to modulate the accessibility of reagents and the coupling efficiency. Here

we demonstrate that the $^{13}$C SSNMR approach allows us to quantify the dynamic properties of the peptide in SPPS. Figure S7(a, b) shows $^{13}$C-$^{1}$H dipolar dephasing curves in $^{13}$C-$^{1}$H REDOR experiments of $^{13}$C$_\alpha$ in (a) Ala-30 and (b) Ala-2 for Aβ(1-40) for the samples solvated with DCM (open circles) and the dried samples (open triangles) in comparison with simulated curves for different order parameters of $S$ = 0.81-0.95 (dotted curves). For Ala-2 and Ala-30, the signal corresponding to the β-strand structure was analyzed. The pulse sequence is shown in Fig. S2. Although more sophisticated pulse sequences are available for accurate measurements of order parameters,[8-9] we used this sequence as a convenient alternative for quantitative analysis. In this experiment, the normalized signal intensity $I(\tau)/I_0$ is decreased by $^{13}$C-$^{1}$H dipolar couplings for rigid solids as the effective dephasing period ($\tau$) is elongated, where $I_0$ = $I(0)$, for which a full echo signal is obtained with little dipolar dephasing (See Fig. S2 for details). In the presence of substantial molecular motions, $^{13}$C-$^{1}$H dipolar couplings are partly averaged out, and scaled down by a factor defined as an order parameter $S$; thus the extent of the dephasing should be considerably less ($S \ll 1$). For rigid solids, there is nearly no scaling (i.e. $S \sim 1$). As discussed above, we originally expected substantial mobility of the peptide chains in DCM. However, as summarized in Table S2, the order parameters $S$ did not show substantial difference between the dry samples ($S$ = 0.91-0.93) and samples solvated in DCM ($S$ =0.84-0.86) for Aβ(1-40) for Ala-2 and Ala-30. The values of $S$ close to 1 suggest that the motional averaging is scarce even in the presence of organic solvents such as DCM. Therefore, it is most likely that Aβ(1-40) that was misfolded into β-strand exhibits little motions over the entire sequence while the N-terminus region retains some population that is considerably dynamic. As discussed above, we also compared $^{13}$C CPMAS spectra of solvated and dry resin-bound Aβ(1-40) samples (Fig. S4). Although line widths for solvated samples are slightly narrower in general, the chemical shift positions and signal intensities are largely unaltered. Similar trends were observed for amyloid fibrils,[10-11] for which only limited motions were observed for their β-strand regions even with solvents. Thus, we concluded that the mobility of the Aβ(1-40) peptides during SPPS is highly restricted. This is the first report showing that highly restricted molecular motions were quantitatively presented with site specificity for a long peptide sequence during SPPS. The restricted motion and β-strand formation in the N-terminus are likely to limit the accessibility of reagents at the peptide terminal as the peptide chain becomes longer.
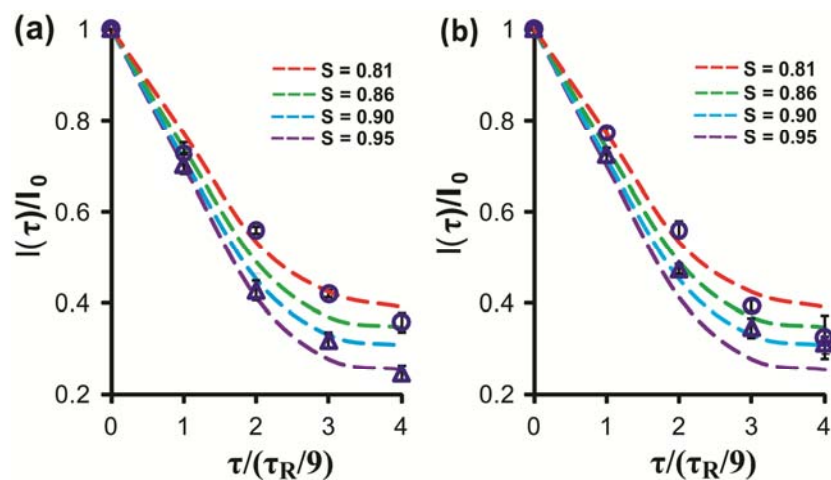
**Figure S7**. The effective dephasing time ($\tau$) dependence of $^{13}C$-$^{1}H$ diplar dephasing curve for $^{13}C_{\alpha}$ of (a) Ala-30 and (b) Ala-2 in A$\beta$(1-40) for the samples solvated with DCM (open circle) and the dried samples (open triangle) in comparison with simulated curves for different order parameters indicated above (dotted lines). In the simulated curves, $^{13}C$-$^{1}H$ distances were assumed to be 1.12 Å, which is 3% longer than the neutron-diffraction distance of H-C$_{\alpha}$ for L-alanine (1.09 Å)[12] by taking account of thermal vibration effects of a C-H group in rigid solids.[13]

**Table S1.** $^{13}$C chemical shifts for isotope-labeled amino acid residues in Aβ(1-40) bound to resin.

| Resides and Sites | | Experimental Chemical Shift (ppm) [a] | Chemical Shift for Random Coil [14] (ppm) | The Difference between Experimental and Theoretical (ppm) | Dihedral Angles from TALOS for Aβ(1-40) Bbond to Resin |
|---|---|---|---|---|---|
| **Ala-2** | Cα | 49.2 | 50.8 | -1.6 | Φ = -142±20 |
| | Cβ | 21.4 | 17.4 | 4.0 | ψ = 149±17 |
| | C=O | 173.1 | 176.1 | -3.0 | |
| | Cα' [b] | 53.7 | 50.8 | 2.9 | Φ = -58±7 |
| | Cβ' | 17.7 | 17.4 | 0.3 | ψ = -43±6 |
| | C=O' | 176.6 | 176.1 | 0.5 | |
| **Phe-4** [d] | Cα | 54.1 | 56.0 | -1.9 | Φ = -132±13 |
| | Cβ | 41.4 | 37.9 | 3.5 | ψ = 153±17 |
| | C=O | 171.2 | 174.1 | -2.9 | |
| | Cα' | 59.4 | 56.0 | 3.4 | Φ = -64±7 [c] |
| | Cβ' | 37.1 | 37.9 | -0.8 | ψ = -44±5 |
| | C=O' | 174.4 | 174.1 | 0.3 | |
| **Val-12** | Cα | 56.5 | 60.5 | -4.0 | Φ = -137±12 |
| | Cβ | 35.1 | 31.2 | 3.9 | ψ = 156±14 |
| | C=O | 171.9 | 174.6 | -2.7 | |
| | Cα' | 65.3 | 60.5 | 4.8 | Φ = -65±5 |
| | Cβ' | 29.2 | 31.2 | -2 | ψ = -41±7 |
| | C=O' | 175.5 | 174.6 | 0.9 | |
| **Phe19** | Cα | 54.2 | 56.0 | -1.8 | Φ = -119±10 |
| | Cβ | 41.3 | 37.9 | 3.4 | ψ = 147±12 |
| | C=O | 172.6 | 174.1 | -1.5 | |
| **Val-24** | Cα | 58.3 | 60.5 | -2.2 | Φ = -134±14 |
| | Cβ | 33.9 | 31.2 | 2.7 | ψ = 153±17 |
| | C=O | 171.9 | 174.6 | -2.7 | |
| **Gly-25** | Cα | 43.6 | 43.4 | 0.2 | Φ = -148±18 [c] |
| | C=O | 169.5 | 173.2 | -3.7 | ψ = 147±26 |
| **Ala-30** | Cα | 49.6 | 50.8 | -1.2 | Φ = -135±11 |
| | Cβ | 22.1 | 17.4 | 4.7 | ψ = 156±18 |
| | C=O | 173.2 | 176.1 | -2.9 | |
| **Leu-34** | Cα | 52.4 | 53.4 | -1.0 | Φ = -132±24 [c] |
| | Cβ | 45.2 | 40.7 | 4.5 | ψ = 137±18 |
| | C=O | 171.4 | 175.9 | -4.5 | |

a) All the $^{13}$C chemical shifts shown above are referenced to TMS. The chemical shifts used for prediction of TALOS were referenced to DSS.

b) The $^{13}$C chemical shifts for $C_\alpha'$, $C_\beta'$ and C=O' (highlighted by green) indicate those for the new peaks which were observed after removal of DCM in Fig. 2c. These peaks are not visible in Fig. 2a.

c) TALOS predictions for theses residues reported 9 best matches from the TALOS database. For the other residues, TALOS reported 10 best matches from the TALOS database

d) The $^{13}$C shifts of the α-helix component of Phe4 were determined by the DARR experiment (Fig. S6).

**Table S2**. The simulation results for order parameter *S* for two Ala in Aβ anchored to a resin support in different conditions.

|  | Order parameter *S* |
|---|---|
| Ala30    (in DCM) | 0.84 |
| Ala30 (Dry) | 0.93 |
| Ala2    (in DCM) | 0.86 |
| Ala2    (Dry) | 0.91 |
| L-alanine (Control) | 0.91 |

**Supplementary Reference:**

(1) Fields, C. G.; Fields, G. B.; Noble, R. L.; Cross, T. A. *International Journal of Peptide and Protein Research* **1989**, *33*, 298.

(2) Chimon, S.; Ishii, Y. *Journal of the American Chemical Society* **2005**, *127*, 13472.

(3) Chimon, S.; Shaibat, M. A.; Jones, C. R.; Calero, D. C.; Aizezi, B.; Ishii, Y. *Nature Structural & Molecular Biology* **2007**, *14*, 1157.

(4) Bennett, A. E.; Rienstra, C. M.; Auger, M.; Lakshmi, K. V.; Griffin, R. G. *J. Chem. Phys.* **1995**, *103*, 6951.

(5) Ishii, Y. *J. Chem. Phys.* **2001**, *114*, 8473.

(6) Veshtort, M.; Griffin, R. G. *J. Magn. Reson.* **2006**, *178*, 248.

(7) Takegoshi, K.; Nakamura, S.; Terao, T. *Chem. Phys. Lett.* **2001**, *344*, 631.

(8) McDermott, A. *Annual Review of Biophysics* **2009**, *38*, 385.

(9) Chevelkov, V.; Xue, Y.; Linser, R.; Skrynnikov, N. R.; Reif, B. *J. Am. Chem. Soc.* **2010**, *132*, 5015.

(10) Jayasinghe, S. A.; Langen, R. *Journal of Biological Chemistry* **2004**, *279*, 48420.

(11) Luca, S.; Yau, W. M.; Leapman, R.; Tycko, R. *Biochemistry* **2007**, *46*, 13505.

(12) Lehmann, M. S.; Koetzle, T. F.; Hamilton, W. C. *J. Am. Chem. Soc.* **1972**, *94*, 2657.

(13) Ishii, Y.; Terao, T.; Hayashi, S. *Journal of Chemical Physics* **1997**, *107*, 2760.

(14) Wishart, D. S.; Bigam, C. G.; Holm, A.; Hodges, R. S.; Sykes, B. D. *J. Biomol. NMR* **1995**, *5*, 67.